Mechanical Systems and Signal Processing (2001) **15**(4), 737–758
doi:10.1006/mssp.2000.1385, available online at http://www.idealibrary.com on IDEAL®

MIMO LMS-ARMAX IDENTIFICATION OF VIBRATING STRUCTURES—PART II: A CRITICAL ASSESSMENT

A. Florakis and S. D. Fassois

Department of Mechanical & Aeronautical Engineering, Stochastic Mechanical Systems (SMS) Group, University of Patras, GR 265 00 Patras, Greece. E-mail: fassois@mech.upatras.gr

F. M. Hemez

Engineering Sciences and Applications, ESA-EA, M/S P946, Los Alamos National Laboratory, Los Alamos, NM 87545, U.S.A. E-mail: hemez@lanl.gov

(Received 13 April 2000, accepted 19 December 2000)

In this part of the paper, a critical assessment of the MIMO (multiple-input multiple-output) LMS-ARMAX method is presented, along with comparisons with a pure ARX version and the Eigensystem Realisation Algorithm (ERA) based upon two-input three-output vibration data obtained from a scale aircraft skeleton structure. This structure is characterised by light ($\zeta < 1\%$) damping and seven modes within the considered frequency range, two of which are closely spaced and another is a 'local' tail mode. The study focuses on the: (i) ability of the methods to handle higher-dimensional problems, (ii) ability to estimate closely spaced and 'local' modes. (iii) ability to accurately estimate light modal damping, (iv) required model overdetermination, (v) distinction of structural from 'extraneous' modes, (vi) effects of various (white/colour) noise environments, and (vii) suitability of various discrete-time representations for effective identification.

The LMS-ARMAX method is shown to be effective, achieving high accuracy in all considered cases. Its various features, such as the stochastic ARMAX representation, the guaranteed stability version, the modest computational complexity and the digital dispersion analysis, are of critical importance. Compared to the pure ARX version, the LMS-ARMAX method is shown to lead to more parsimonious representations and overall better model fits. The ERA is shown to lag behind in terms of overall performance, leading to somewhat lower accuracy, in particular for the two closely spaced modes, and encountering difficulties in distinguishing structural modes via the modal amplitude coherence (MAC).

1. INTRODUCTION

In the first part of this paper [1], a comprehensive linear multi stage autoregressive moving average with exogenous excitation (LMS-ARMAX) method for stochastic multiple-input multiple-output (MIMO) structural identification was introduced. The method consists of (a) a vector ARMAX representation of an appropriate form, (b) effective LMS parameter estimation, (c) statistical order selection/validation, and (d) a digital dispersion analysis (DA) methodology for effective modal characterisation. The LMS-ARMAX method overcomes many of the difficulties that had rendered MIMO ARMAX identification difficult in the past, featuring modest computational complexity, high accuracy, guaranteed algorithmic and model stability, and thus applicability to higher-dimensional problems and lightly damped structures, accurate modal parameter extraction and effective distinction of structural from 'extraneous' modes.

0888–3270/01/040737 + 22 $35.00/0

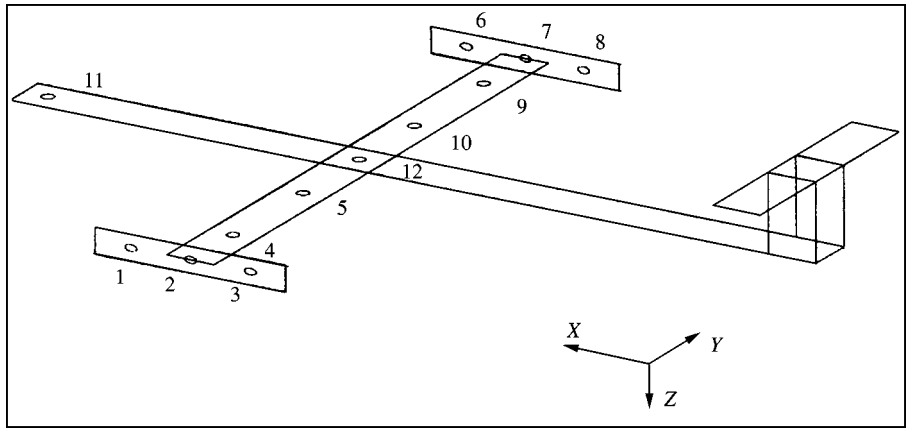

Figure 1. Schematic of the aircraft skeleton structure.

In the present part of the paper, a critical assessment of the LMS-ARMAX method, as well as comparisons with a simpler pure ARX version and the Eigensystem Realisation Algorithm (ERA) [2, 3], are presented. These are based upon experimental vibration data from a scale aircraft skeleton structure, which is characterised by seven modes within the considered frequency range, light modal damping ($\zeta < 1\%$), a pair of closely spaced (frequency separation smaller than 0.1 Hz) modes and a 'local' (tail bending) mode [4]. The study focuses on some of the practically important, but generally less explored, technical issues [5], such as

(i) ability of the methods to handle *higher-dimensional* problems;
(ii) ability of the methods to accurately identify *all* modes, including *closely spaced* ones;
(iii) ability of the methods to identify '*local*' modes from 'remote' measurements;
(iv) ability of the methods to accurately estimate *light* modal damping;
(v) the role, required degree and consequences of model *overdetermination*;
(vi) ability of the methods to *distinguish* between structural and 'extraneous' modes;
(vii) ability of the methods to operate under various *noise* environments (white/colour noise at various levels);
(viii) suitability of different *discrete-time representations* for effective identification.

The presentation in this part of the paper is organised as follows. A description of the test structure under study is given in Section 2. LMS-ARMAX-based structural identification results are presented in Section 3, along with critical comparisons with a pure ARX version and the ERA. A discussion on the results is presented in Section 4, and concluding remarks are summarised in Section 5.

2. DESCRIPTION OF THE TEST STRUCTURE AND EXPERIMENT

The structure under test consists of the reduced model of an airplane skeleton (Fig. 1) designed and manufactured by ONERA (France) in conjunction with the Structures and Materials Action Group SM-AG-19 of the Group for Aeronautical Research and Technology in Europe (GARTEUR) (see reference [6]). The model's fuselage, wings and tail are constructed from standard aluminium beams, jointed together through bolted connections.

TABLE 1

Dimensions of the scale aircraft skeleton structure

Component	Length (m)	Width (m)	Thickness (m)
Fuselage	1.50	0.15	0.025
Wings	2.00	0.10	0.015
Tail	0.40	0.10	0.015

TABLE 2

Modes obtained by force appropriation

Mode no.	Frequency (Hz)	Damping ratio (%)	Description
1	6.14	0.59	Sym. wing bending (2 nodes)
2	16.44	0.85	Skew-sym. tail bending
3	35.87	0.47	Skew-sym. wing bending (3 nodes)
4	39.41	n/a†	Right wing torsion
5	39.47	n/a†	Left wing torsion
6	44.14	0.46	Sym. wing bending (4 nodes)

† Not available.

The structure weighs 44 kg, while the fuselage is 1.5 m long and the wingspan is 2 m long. The structure's main dimensions are indicated in Table 1.

As bolted aluminium structures are characterised by very light damping, additional energy dissipation was introduced through the use of an acrylic viscoelastic layer with an aluminium constraining layer. Suspension was provided through a set of bungee cords linked to a small plate and designed in such a way as to exhibit a pendulum rigid body mode below the frequency range of interest. The boundary conditions thus were free–free.

The experimental data used in this study were obtained at SOPEMEA (France). The skeleton structure was excited through modal shakers applying random force excitation along the vertical z-axis at two symmetrical locations on the wings (nodes 4 and 9, Fig. 1). The applied force excitation was measured through load cells, while the resulting vibration accelerations were measured via accelerometers along the vertical z-direction at 12 locations symmetrically distributed on the wings and the tip of the fuselage (nodes 1–12, Fig. 1).

The structure's modal characteristics in the frequency range 5–50 Hz, as determined by force appropriation, are presented in Table 2. Given the carefully controlled test environment, the accuracy of the obtained frequencies is considered to be within 0.1 Hz. Based on these characteristics, the challenging features of this structure are: (a) its light damping ($\zeta < 1\%$)—a characteristic common in aerospace structures which makes accurate damping estimation difficult [7]; (b) a pair of closely spaced modes (modes 4 and 5, in the neighbourhood of 39.4 Hz with frequency separation smaller than 0.1 Hz); and (c) a 'local' tail bending mode (mode 2), whose identification is challenging due to the lack of direct tail measurement or excitation.

3. IDENTIFICATION RESULTS

Structural identification is based upon two-input (random forces applied at nodes 4 and 9) and three-output (resulting vibration accelerations measured at nodes 2, 6 and 10)

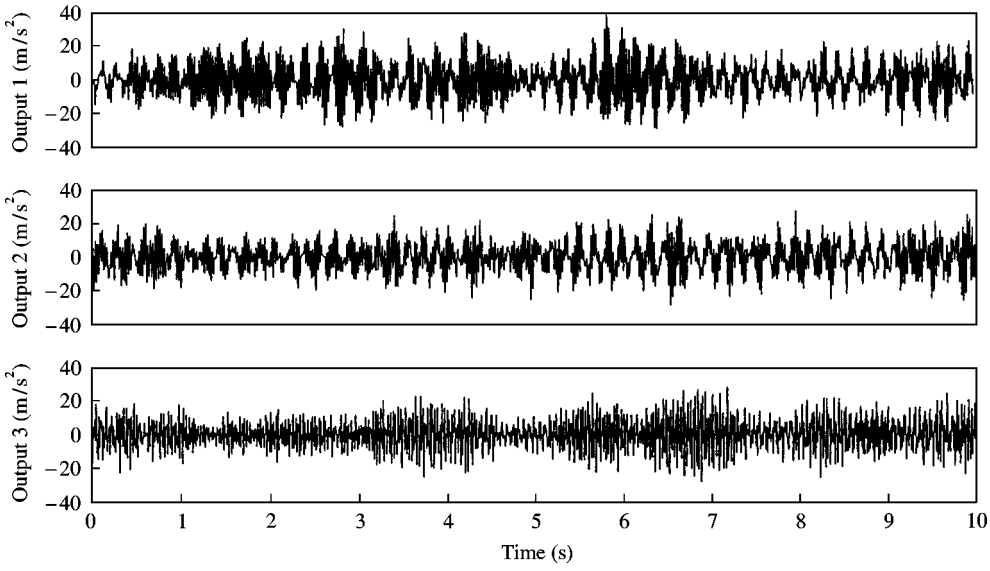

Figure 2. Measured acceleration signals (nodes 2, 6 and 10).

records, each one being $\sim$10 s long. All signals are digitised at 410.0041 Hz, low-pass filtered by using a 15th-order Chebyshev type II filter with cut-off frequency at 75 Hz, re-sampled at $f_s = 205.00205$ Hz, and mean-corrected (mean values subtracted). Each resulting signal is $N = 2048$ samples long. The final vibration responses used in the identification are depicted in Fig. 2. The frequency range of interest is selected as 5–75 Hz, with the lower limit set in order to avoid instrument dynamics.

In LMS-ARMAX identification, stages 3 and 4 of the estimation (see Part I) are iterated, with the estimate corresponding to minimum trace of the estimated innovations covariance selected as best. Moreover, the guaranteed stability version of the algorithm is used as necessary. On the other hand, ARX identification is based along the exact same lines as LMS-ARMAX identification, with the only difference being the explicit constraint of the model to the special ARX form. ERA identification is based upon the transformation of the random input/output signals into corresponding Markov parameter estimates [3]. The generalised Hankel matrix (see Appendix A and reference [3]) consists of $\alpha \times \beta = 100 \times 50$ submatrices, with each Markov parameter being of dimensions $p \times r = 3 \times 2$. This results in overall Hankel matrix dimensions of $\alpha p \times \beta r = 300 \times 100$.

In all cases the degree of overdetermination, defined as the number of model poles over the number of actual structural poles, is computed for the selected model, along with the number of data samples per estimated model parameter (SPP).

Three cases are considered: *Test Case I* with no extra noise added on the response measurements, *Test Case II* with 10% (variance ratio) added white noise and *Test Case III* with 10% (variance ratio) added colour noise.

3.1. TEST CASE I: NO ADDED NOISE

3.1.1. ARMAX identification

Although a fifth-order 3-dimensional (3-D) model is theoretically sufficient for capturing all structural modes within the considered frequency range, such a model proves inadequate

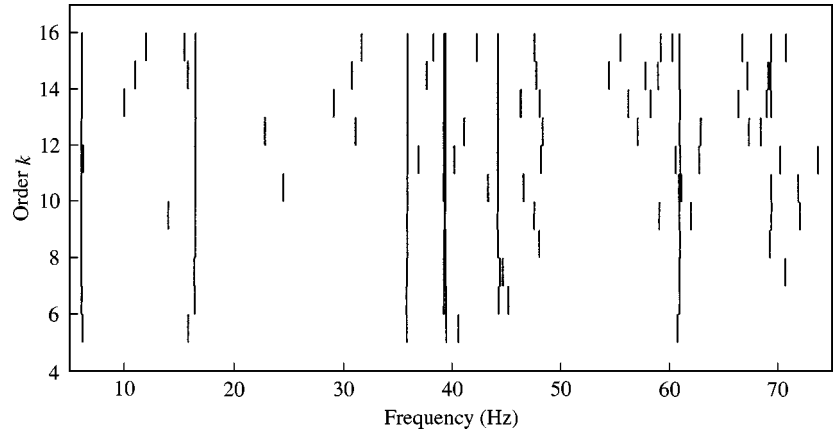

Figure 3. Frequency stabilisation diagram [ARMAX(k, k, nc) models; no added noise].

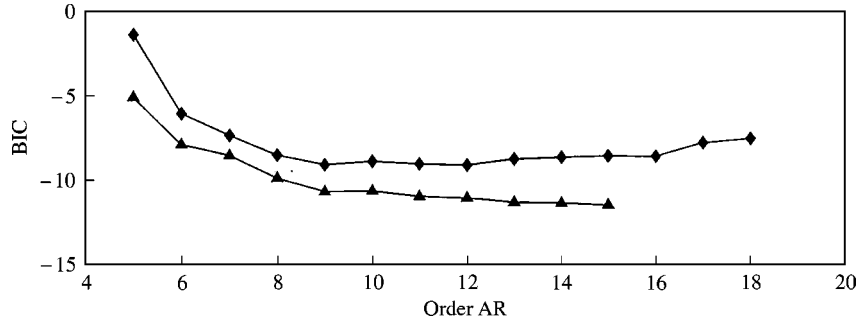

Figure 4. BIC *vs* AR order ($\diamond$: ARX models; $\triangle$: ARMAX models; no added noise).

in providing accurate modal estimates. The estimation of ARMAX(k, k, l) models with $k = 5, 6, 7, \ldots$ reveals that only for $k \geqslant 11$ is 'stabilisation' of modal frequencies and modal dispersions, combined with accurate estimation of modal damping ($\zeta < 1\%$), achieved (partial results in Fig. 3). The BIC (see Part I) indicates that the ARMAX(15, 15, 2) model should be selected as adequate (see Fig. 4); a result supporting the previous observation and underlining the need for drastic overdetermination. Yet, for purposes of 'economy', the lower order ARMAX(11, 11, 14) model, which is characterised by minor differences from the former, is selected. It should be noted that the degree of overdetermination for this model is 136%, and the number of data samples per estimated model parameter (SPP) is 34.5.

The ARMAX(11, 11, 14)-based modal parameters are, for the considered frequency range, presented in Table 3, along with their corresponding dispersion matrix norms ($\|\Delta\|$). The results indicate the presence of seven significant ($\|\Delta\| > 3\%$) modes. The first six are essentially identical to those obtained by force appropriation, including the local tail (mode 2) and the two closely spaced modes (modes 4 and 5). The seventh mode, being beyond the range explored by force appropriation, is at 61.04 Hz and is characterised by a strong (35.40%) dispersion norm. These results demonstrate the effectiveness of the dispersion analysis (DA) methodology in distinguishing the actual from 'extraneous' modes.

The force appropriation and the ARMAX(11, 11, 14) model-based frequencies are pictorially compared in Fig. 5, where the complete dominance (in terms of modal dispersions) of

TABLE 3

No added noise case: *force appropriation*, $ARMAX(11,11,14)$, $ARX(12,12)$, *and* $ERA(28)$ *modes in the frequency range* 5–75 Hz (2 *inputs*, 3 *outputs*; *ARMAX and ARX modes with* $\|\Delta\| > 3\%$ *are in bold face*)

Force appropriation		ARMAX modes†			ARX modes†			ERA modes†		
ω_n (Hz)	ζ (%)	ω_n (Hz)	ζ (%)	$\|\Delta\|$ (%)	ω_n (Hz)	ζ (%)	$\|\Delta\|$ (%)	ω_n (Hz)	ζ (%)	*MAC* (%)
6.14	0.59	**6.16**	**0.80**	**52.41**	**6.16**	**0.70**	**53.83**	6.04	2.69	99.92
								7.24	− 4.27	97.28
16.44	0.85	**16.45**	**0.46**	**8.75**	**16.45**	**0.41**	**8.82**	16.38	0.40	99.71
					31.64	26.10	0.04			
								33.25	1.57	96.38
								34.31	0.22	95.45
35.87	0.47	**35.90**	**0.50**	**52.82**	**35.88**	**0.51**	**60.54**	35.81	0.58	99.72
		36.90	53.35	0.61						
39.41	n/a	**39.22**	**0.85**	**32.69**	**39.24**	**0.89**	**36.51**	39.02	0.62	99.65
39.47	n/a	**39.39**	**0.47**	**42.93**	**39.39**	**0.52**	**46.71**	39.40	0.30	99.96
		40.20	20.90	0.65						
44.14	0.46	**44.24**	**0.57**	**7.41**	**44.22**	**0.59**	**8.46**	44.36	0.23	99.82
		48.23	2.66	0.61	47.82	3.98	0.63			
					52.76	19.17	0.41			
					55.15	5.01	0.16			
					57.38	10.35	0.95			
		60.65	35.66	0.36				60.00	0.32	99.74
n/a	n/a	**61.04**	**0.73**	**35.40**	**61.02**	**0.68**	**35.08**			
								61.90	1.14	99.74
		62.78	5.32	0.75						
					66.01	1.60	0.04			
					69.70	2.11	0.07			
		70.24	1.26	0.00	70.08	1.98	0.01			
		73.71	6.45	0.03						
Overdetermination			136%			157%			100%	
No. of pars/SPP			297/34.5			186/55.1			924/11.1	

† Only complex poles are shown.
Note: n/a, not available; no. of pars, number of estimated parameters; SPP, samples per parameter.

the seven estimated modes and their agreement with their force appropriation counterparts is evident. The estimated damping ratios (Table 3) are all below 1%, and in good agreement with those provided by force appropriation; a fact quite remarkable in view of the low level of damping and the consequent estimation difficulties [7]. The ARMAX(11, 11, 14)-based frequency response magnitude curves are presented in Fig. 6. For purposes of comparison, corresponding non-parametric estimates obtained by vector spectral analysis via the Blackman–Tukey frequency domain procedure [8] (512-sample-long segments and Hamming windowing are used) are presented in Fig. 7. The two estimates are in rough qualitative agreement, with the superior quality of the ARMAX(11, 11, 14) curves being evident.

The representation accuracy provided by the ARMAX(11, 11, 14) model may be additionally confirmed via comparisons of model-based simulations with the actual (measured) structural vibrations. These are, for all three outputs, presented in Fig. 8 and clearly illustrate excellent agreement between the two types of curves.

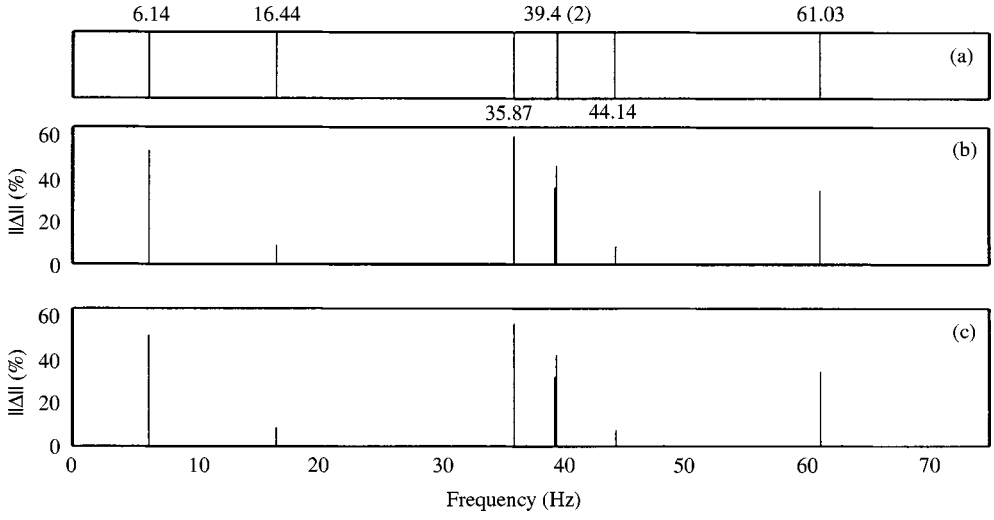

Figure 5. (a) Force appropriation-based frequencies; (b) ARX(12, 12)-based frequencies and dispersion norms; (c) ARMAX(11, 11, 14)-based frequencies and dispersion norms (no added noise).

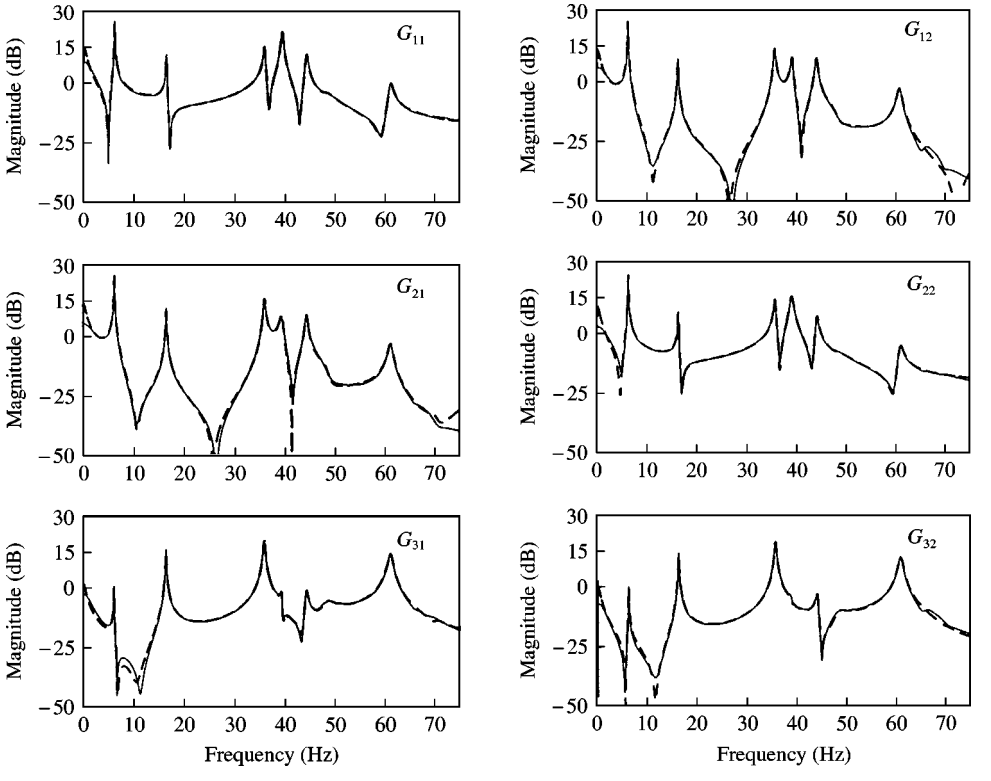

Figure 6. Estimated frequency response magnitude curves (- - -: ARMAX(11, 11, 14); —: ARX(12, 12); no added noise).

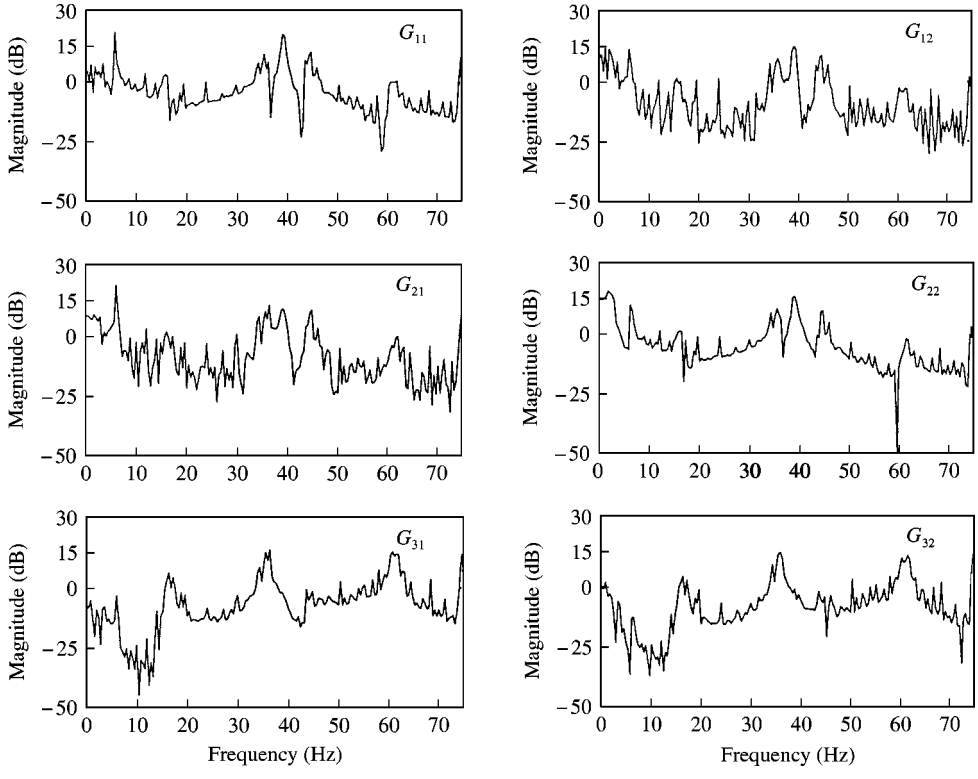

Figure 7. Non-parametrically estimated frequency response magnitude curves (Blackman–Tukey method; no added noise).

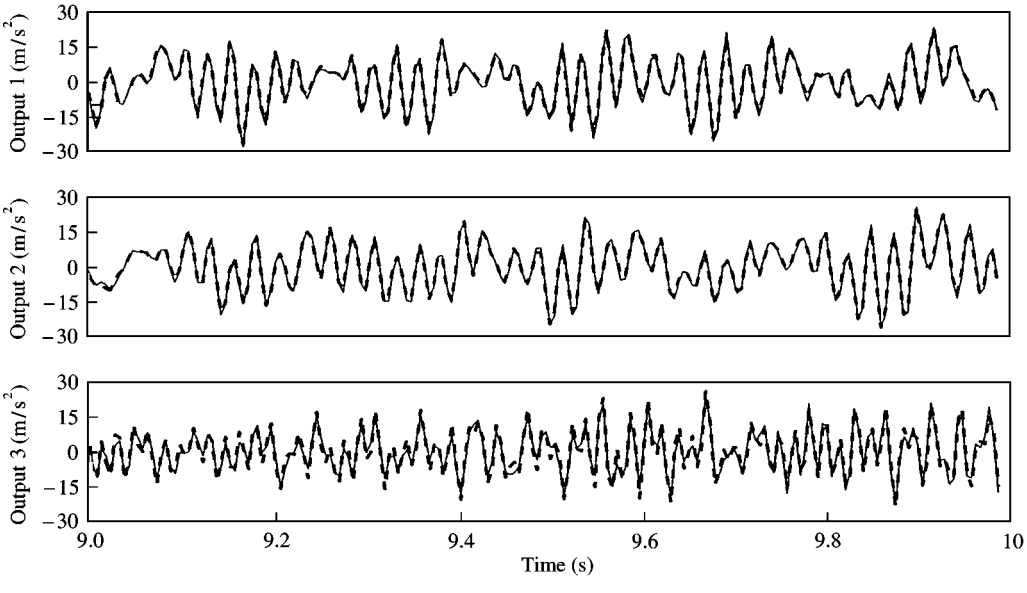

Figure 8. Actual (—) and ARMAX(11, 11, 14) simulated (- - -) outputs (no added noise).

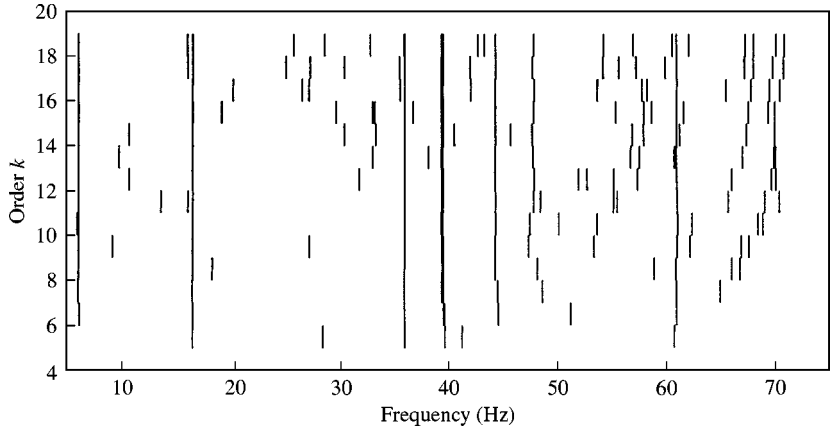

Figure 9. Frequency stabilisation diagram [ARX(k, k) models; no added noise].

3.1.2. *ARX identification*

Like in the ARMAX case, a fifth-order model proves inadequate in providing accurate modal estimates. The estimation of ARX(k, k) models with $k = 5, 6, 7, \ldots$ reveals that only for $k \geqslant 11$ is 'stabilisation' of modal frequencies and modal dispersions, combined with accurate estimation of modal damping ($\zeta < 1\%$), achieved (partial results in Fig. 9). The BIC indicates that the ARX(12, 12) model should be selected as adequate (see Fig. 4). The degree of overdetermination for this model is 157%, and the number of data samples per estimated model parameter (SPP) is 55.1.

The ARX(12, 12)-based modal parameters are, for the considered frequency range, presented in Table 3 as well, along with their corresponding dispersion matrix norms ($\|\Delta\|$). The results indicate the presence of seven significant ($\|\Delta\| > 3\%$) modes, which are very close to those estimated via the ARMAX(11, 11, 14) model. The force appropriation and the ARX(12, 12) model-based frequencies are also compared in Fig. 5, where the complete dominance (in terms of modal dispersions) of the seven estimated modes and their agreement with their force appropriation counterparts is evident. The estimated damping ratios are all below 1%, and in good agreement with those provided by force appropriation. The ARX(12, 12)-based frequency response magnitude curves are presented in Fig. 6, where good agreement with their ARMAX(11, 11, 14) counterparts is observed.

The only essential difference between the ARX(12, 12) and the ARMAX(11, 11, 14) results in the present case is the somewhat higher degree of overdetermination necessitated by the former model, and the resulting higher number of 'extraneous' modes within the considered frequency range. These are, nevertheless, effectively distinguished by the dispersion analysis (DA) methodology (Table 3). Worth observing also is the fact that the estimated ARMAX models achieve, in their entity, better 'fits' than their ARX counterparts; this is clearly reflected in the lower BIC values attained (Fig. 4) despite the BIC built-in penalty associated with their higher parametrisation complexity.

3.1.3. *ERA identification*

The singular value decomposition of $\mathbf{H}[0]$ (see Appendix A) appears to indicate a number of possible model orders (Fig. 10). Yet, the 'lower' order models fail to properly identify both of the structure's closely spaced modes (modes 4 and 5), and are thus inadequate. The

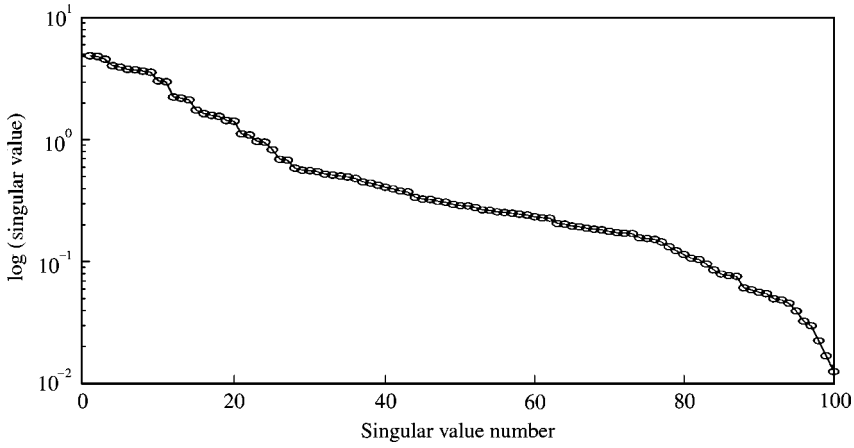

Figure 10. Singular values of the estimated Hankel matrix (ERA; no added noise).

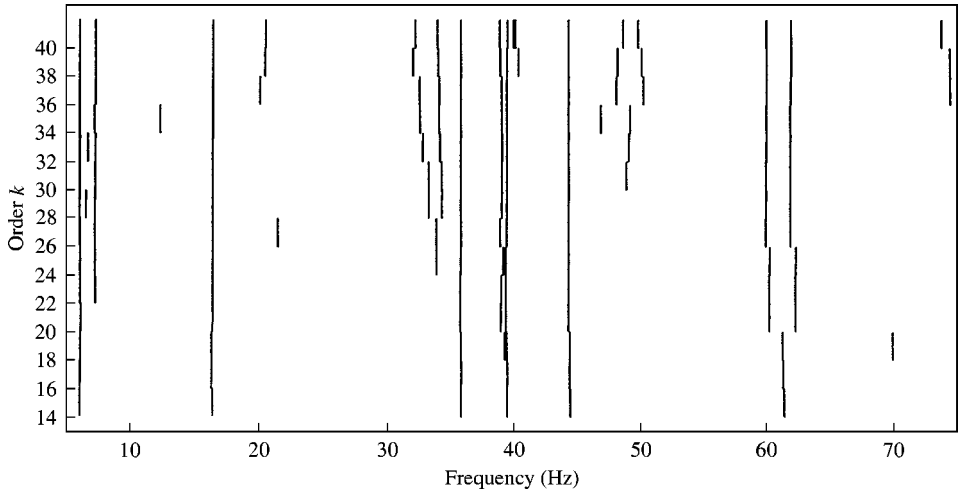

Figure 11. Frequency stabilisation diagram (ERA; no added noise).

use of modal frequency stabilisation diagrams (Fig. 11) suggests that models of order 28 or higher are necessary for this purpose, and a state-space model of order $n = 28$ is selected. The degree of overdetermination in this case is 100%, and the number of data samples per estimated model parameter (SPP) is 11.1.

The ERA-based modal parameters are, for the considered frequency range, presented in Table 3 as well, along with the corresponding modal amplitude coherence (MAC) values. The first six structural modes are estimated, but the agreement with the force appropriation results is not as good as in the ARMAX and ARX cases, and the first of the two closely spaced modes (mode 4) is underestimated. The seventh mode is not properly estimated, although neighbouring modes (at 60.00 and 61.90 Hz are obtained). Furthermore, the estimated model is unstable, and the distinction of structural from 'extraneous' modes is inadequate, as the latter appear characterised by high MAC values as well (Table 3). Finally, damping levels are accurately estimated, although that of mode 1 is overestimated (at 2.69%).

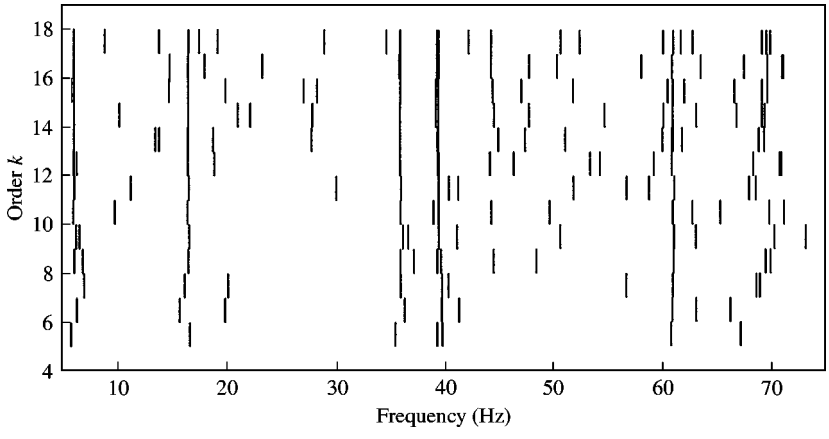

Figure 12. Frequency stabilisation diagram [ARMAX(k, k, nc) models; 10% added white noise].

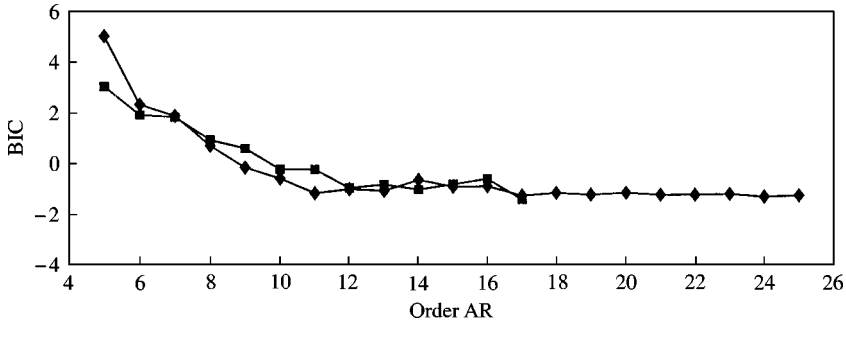

Figure 13. BIC *vs* AR order (◇: ARX models; □: ARMAX models; 10% added white noise).

3.2. TEST CASE II: 10% ADDED WHITE NOISE

In this case, the methods' performance characteristics are investigated under additional noise superimposed on the measured vibration acceleration signals. The superimposed noise is random, zero-mean, with flat spectrum in the 0–75 Hz frequency range (low-pass filtered white noise). The noise-to-signal (N/S) variance ratio in each output channel is 10%.

3.2.1. ARMAX identification

As in Test Case I, fifth-order models prove inadequate in capturing all structural modes. The estimation of ARMAX(k, k, l) models with $k = 5, 6, 7, \ldots$ reveals that only for $k \geqslant 16$ is 'stabilisation' of modal frequencies and modal dispersions, combined with accurate estimation of modal damping ($\zeta < 1\%$), achieved (partial results in Fig. 12). Note, however, that some of the 'extraneous' frequencies tend to also 'stabilise' in this case; a fact implying the increased caution that needs to be exercised. In line with these observations, model adequacy (based upon the BIC) is achieved for the ARMAX(17, 17, 2) model (Fig. 13). Yet, for purposes of 'economy', the lower order ARMAX(16, 16, 20) model is selected. The degree of overdetermination in this case is 243%, and the number of data samples per estimated model parameter (SPP) is 24.0.

The ARMAX(16, 16, 20)-based modal parameters are, for the considered frequency range, presented in Table 4, along with their corresponding dispersion matrix norms. The results clearly indicate the presence of seven significant ($\|\Delta\| > 3\%$) modes which are in close agreement with those identified in Test Case I and also with those obtained through force appropriation (also see Fig. 14). The estimated damping ratios are all in good agreement with those provided by force appropriation, with only that of mode 4 slightly exceeding 1%. The only essential 'complication' caused by the added noise in this case is the higher overdetermination necessitated and the resulting higher number of extraneous modes; these are, nevertheless, effectively distinguished by the digital dispersion analysis (DA).

The ARMAX(16, 16, 20)-based frequency response magnitude curves are in close agreement with those obtained in Test Case I, and the model-based simulations are also in agreement with the actual (measured) structural vibrations.

3.2.2. ARX identification

Similar to the ARMAX case, the estimation of ARX(k, k) models with $k = 5, 6, 7, \ldots$ leads to high-order representations. 'Stabilisation' of modal frequencies and modal dispersions, combined with accurate estimation of modal damping, is achieved for $k \geqslant 18$ (partial results in Fig. 15). 'Stabilisation' is more problematic than in the corresponding ARMAX case, as the number of 'extraneous' modes tends to be higher and some of them exhibit a 'stabilising' behaviour. Model adequacy (based upon the BIC) is achieved for the ARX(24, 24) model (Fig. 13); yet the more 'economical' ARX(18, 18) model is selected. The degree of overdetermination in this case is 286%, and the number of data samples per estimated model parameter (SPP) is 37.1.

The ARX(18, 18)-based modal parameters are, for the considered frequency range, presented in Table 4 as well, along with their corresponding dispersion matrix norms. The results clearly indicate the presence of seven significant ($\|\Delta\| > 3\%$) modes which are in close agreement with those identified in Test Case I and also with those obtained through force appropriation (also see Fig. 14). The estimated damping ratios are all in good agreement with those provided by force appropriation, with only that of mode 4 exceeding 1%. An essential difference from the ARMAX case is the higher overdetermination necessitated, and the resulting higher number of extraneous modes; many of which in this case have somewhat higher dispersion norms (see Table 4 and Fig. 14). This drawback is due to the inherent difficulty of the ARX models to deal with noise-corrupted signals; a situation much better dealt with complete ARMAX models. It should be, nevertheless, stressed that the structural modes are still properly distinguished by the digital dispersion analysis (DA).

The ARX(18, 18)-based frequency response magnitude curves are in good overall agreement with their ARMAX(16, 16, 20) counterparts, and the model-based simulations are also in agreement with the actual structural vibration.

3.2.3. ERA identification

Like in Test Case I, the 'lower' order models prove inadequate as they fail to identify both of the structure's closely spaced modes (modes 4 and 5). The use of modal frequency stabilisation diagrams (Fig. 16) suggests that models of order 32 or higher are necessary for this purpose. Yet, 'stabilisation' is now more problematic, as several of the 'extraneous' modes tend to exhibit a 'stabilising' behaviour. A state-space model of order $n = 32$ is finally selected. This is characterised by degree of overdetermination equal to 129%. The number of data samples per estimated model parameter (SPP) is quite low, at 8.7.

The ERA-based modal parameters are, for the considered frequency range, presented in Table 4 as well, along with the corresponding modal amplitude coherence (MAC) values.

TABLE 4

Ten per cent added white noise case: force appropriation, ARMAX(16, 16, 20), ARX(18, 18), and ERA(32) modes in the frequency range 5–75 Hz (2 inputs, 3 outputs; ARMAX and ARX modes with $\|\Delta\| > 3\%$ are in bold face)

Force appropriation		ARMAX modes†			ARX modes†			ERA modes†		
ω_n (Hz)	ζ (%)	ω_n (Hz)	ζ (%)	$\|\Delta\|$ (%)	ω_n (Hz)	ζ (%)	$\|\Delta\|$ (%)	ω_n (Hz)	ζ (%)	*MAC* (%)
								5.41	− 4.37	50.80
6.14	0.59	**6.15**	**0.87**	**43.87**	**6.16**	**0.82**	**59.95**	6.10	2.72	98.66
					7.46	91.25	1.98			
		14.78	30.24	0.31	14.65	24.39	0.43			
16.44	0.85	**16.43**	**0.62**	**5.64**	**16.45**	**0.49**	**7.99**	16.35	0.42	99.55
		17.92	54.60	0.40	17.34	23.78	0.71			
		23.18	13.42	0.33						
					25.25	13.48	0.37			
					26.70	13.76	0.22			
								31.72	1.17	97.83
								33.59	− 0.22	96.77
		35.78	30.50	0.39						
35.87	0.47	**35.88**	**0.60**	**60.43**	**35.87**	**0.59**	**59.93**	35.82	0.44	99.54
					37.05	16.34	1.82			
39.41	n/a	**39.22**	**1.10**	**31.33**	**39.23**	**1.30**	**33.02**	38.84	0.41	99.49
39.47	n/a	**39.41**	**0.46**	**39.60**	**39.38**	**0.48**	**45.15**	39.41	0.27	99.94
44.14	0.46	**44.26**	**0.75**	**7.16**	**44.32**	**0.99**	**5.28**	44.34	0.34	99.30
					45.92	6.93	1.43			
		47.81	3.28	0.77						
								48.25	2.76	61.90
		50.41	11.86	1.16	49.85	6.57	1.07			
					55.79	4.07	1.55			
		58.12	4.19	0.43						
					59.48	4.79	2.75	59.79	2.21	97.57
								59.84	0.23	99.70
n/a	n/a	**60.95**	**0.78**	**35.76**	**61.01**	**0.63**	**35.45**			
					62.59	11.65	1.03	62.25	0.84	99.78
		63.57	2.71	0.42	62.94	4.31	0.13			
					64.32	2.79	0.93			
		67.57	2.64	0.21						
		69.70	1.08	0.07	69.63	1.34	0.07			
					70.16	1.68	0.04			
					70.21	0.72	0.07			
		71.03	1.11	0.10						
		71.15	20.66	1.12						
Overdetermination			243%			286%			129%	
No. of pars/SPP			426/24.0			276/37.1			1184/8.7	

† Only complex poles are shown.

Note: n/a, not available; no. of pars, number of estimated parameters; SPP, samples per parameter.

The first six structural modes are estimated, although the distance between modes 4 and 5 is increased, and (like in Test Case I) the damping of mode 1 is overestimated (at 2.72%). The seventh mode is, again, not properly estimated; although some 'neighbouring' frequencies are obtained. Furthermore, like in Test Case I, the estimated model is unstable and the

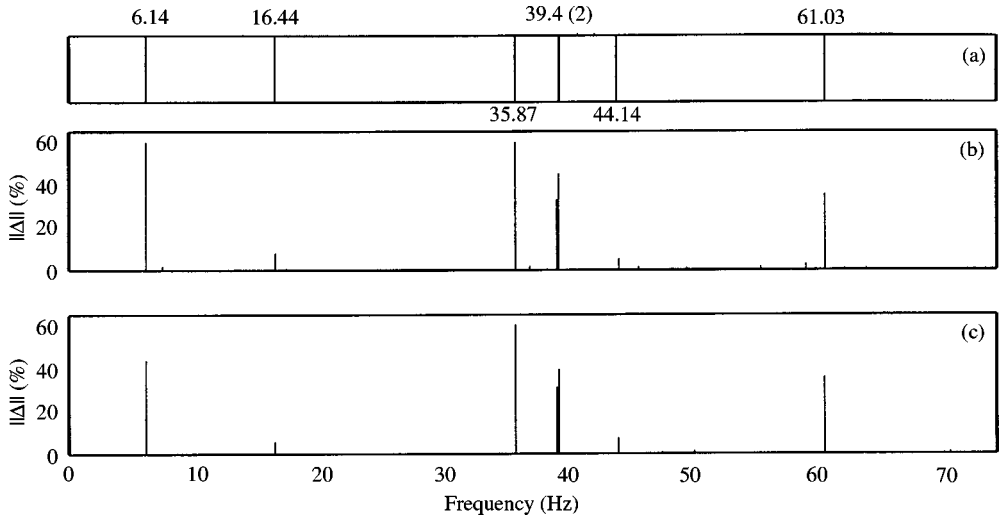

Figure 14. (a) Force appropriation-based frequencies; (b) ARX(18, 18)-based frequencies and dispersion norms; (c) ARMAX(16, 16, 20)-based frequencies and dispersion norms (10% added white noise).

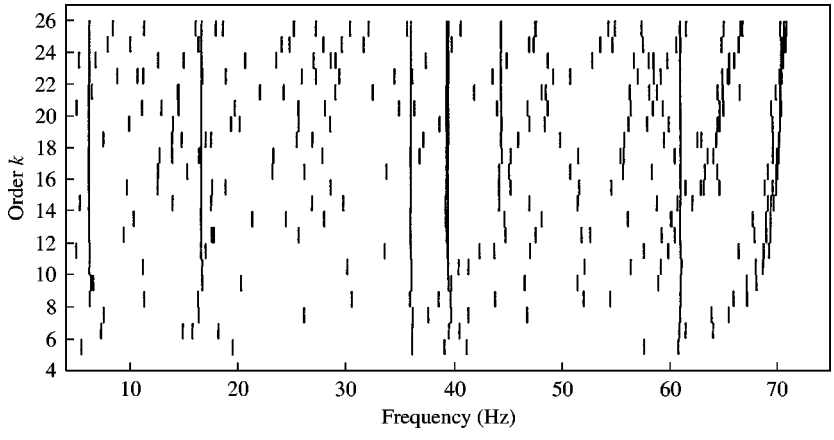

Figure 15. Frequency stabilisation diagram [ARX(k, k) models; 10% added white noise].

distinction of structural from 'extraneous' modes is inadequate as the latter appear characterised by high MAC values as well (Table 4).

3.3. TEST CASE III: 10% ADDED COLOUR NOISE

In this case, the methods' performance characteristics are investigated under colour noise superimposed on the measured vibration acceleration signals. The noise is random, zero-mean band-limited in the 0–75 Hz frequency range, and characterised by natural frequencies $\omega_{n1} = 30$ Hz ($\zeta_1 = 0.8\%$) and $\omega_{n2} = 50$ Hz ($\zeta_2 = 0.7\%$). Like in Test Case II, the noise-to-signal (N/S) variance ratio in each output channel is maintained at 10%. The additional challenge in this case thus is the problem of distinguishing the noise frequencies from those of the structure.

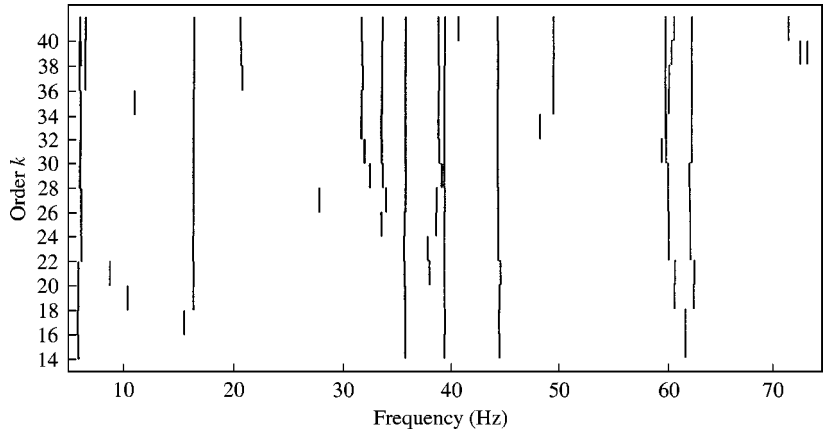

Figure 16. Frequency stabilisation diagram (ERA; 10% added white noise).

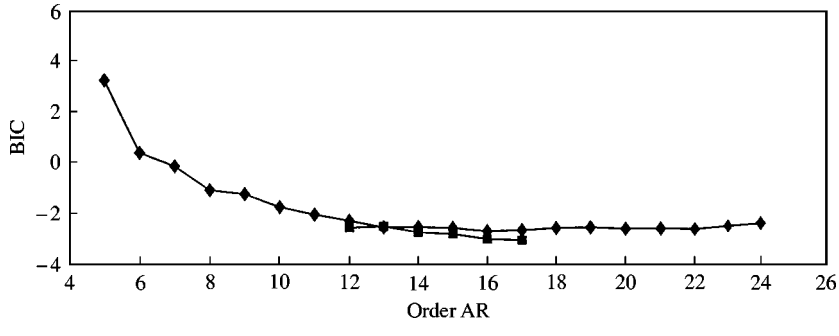

Figure 17. BIC *vs* AR order (◇: ARX models; □: ARMAX models; 10% added colour noise).

3.3.1. ARMAX identification

The estimation of ARMAX(k, k, l) models with $k = 5, 6, 7, \ldots$ reveals that only for $k \geqslant 16$ is 'stabilisation' of modal frequencies and modal dispersions combined with accurate estimation of modal damping ($\zeta < 1\%$), achieved. The problems with 'extraneous' frequencies tending to stabilise are even more pronounced in this case, with the noise frequencies undertaking dominant roles. Model adequacy (based upon the BIC) is achieved for the ARMAX$(17, 17, 1)$ model, although the more 'economical' ARMAX$(16, 16, 1)$ model is selected. The degree of overdetermination in this case is 243%, and the number of data samples per estimated model parameter (SPP) is 40.2.

The ARMAX$(16, 16, 1)$-based modal parameters are, for the considered frequency range, presented in Table 5, along with their corresponding dispersion matrix norms. The results clearly indicate the presence of seven significant ($\|\Delta\| > 3\%$) modes which are in close agreement with those identified in the previous test cases and also obtained through force appropriation (also see Fig. 18). The estimated damping ratios are all in good agreement with those provided by force appropriation, with only those of modes 4 and 6 slightly exceeding 1%. All 'extraneous' modes, including the two noise modes at 30 and 50 Hz, are clearly identified as such by the digital dispersion analysis (DA) (notice that only one 'extraneous' mode is characterised by dispersion norm somewhat higher than 1%).

TABLE 5

Ten per cent added colour noise case: force appropriation, ARMAX(16, 16, 1), *ARX*(20, 20), *and ERA*(44) *modes in the frequency range* 5–75 Hz (2 *inputs*, 3 *outputs*; *ARMAX and ARX modes with* $\|\Delta\| > 3\%$ *are in bold face*)

Force appropriation		ARMAX modes†			ARX modes†			ERA modes†			
ω_n (Hz)	ζ (%)	ω_n (Hz)	ζ (%)	$\|\Delta\|$ (%)	ω_n (Hz)	ζ (%)	$\|\Delta\|$ (%)	ω_n (Hz)	ζ (%)	*MAC* (%)	
6.14	0.59	**6.16**	**0.71**	**33.05**	**6.16**	**0.69**	**40.70**	6.06	3.71	99.43	
								7.23	1.48	81.06	
		14.83	89.21	0.59							
16.44	0.85	**16.44**	**0.47**	**6.65**	**16.44**	**0.45**	**6.36**	16.37	0.51	99.59	
		20.63	35.75	0.08	20.44	28.36	0.01				
					25.44	27.53	0.05				
		29.81	2.21	0.07	29.85	1.02	0.07				
		30.13	1.03	0.19	30.16	0.66	0.02	30.23	0.73	95.57	⇐ Noise mode *a*
								33.45	0.29	96.73	
					35.75	12.98	0.71				
35.87	0.47	**35.87**	**0.58**	**39.24**	**35.88**	**0.57**	**37.69**	35.74	0.36	99.26	
								38.06	16.87	73.27	
					39.00	83.15	0.38				
39.41	n/a	**39.24**	**1.24**	**25.35**	**39.24**	**1.03**	**21.94**	38.67	2.22	94.87	
39.47	n/a	**39.35**	**0.50**	**27.10**	**39.39**	**0.52**	**31.00**	39.38	0.25	99.77	
44.14	0.46	**44.34**	**1.12**	**3.01**	**44.37**	**0.80**	**3.33**	44.39	0.24	99.87	
					49.18	5.81	0.42				
		49.96	1.57	1.13	49.87	0.90	0.46				
		50.10	0.82	0.22	50.13	1.13	0.48	50.23	0.15	99.25	⇐ Noise mode *b*
		50.70	9.48	0.65				50.44	4.15	90.65	
					54.44	8.08	0.15				
					58.96	3.34	0.62				
		60.22	9.47	0.44				60.06	0.52	99.66	
n/a	n/a	**61.03**	**0.63**	**29.32**	**61.00**	**0.64**	**26.94**				
		62.38	15.54	0.84	61.64	7.49	0.22	61.99	1.19	99.71	
		66.29	5.12	0.14							
		68.27	4.48	0.18							
					69.37	2.06	0.06				
					69.41	5.41	0.05				
					70.74	8.43	0.51				
		74.17	6.96	0.99							
Overdetermination			243%			329%			214%		
No. of pars/SPP			255/40.2			306/33.5			2156/4.8		

† Only complex poles are shown.

Note: n/a, not available; no. of pars, number of estimated parameters; SPP, samples per parameter.

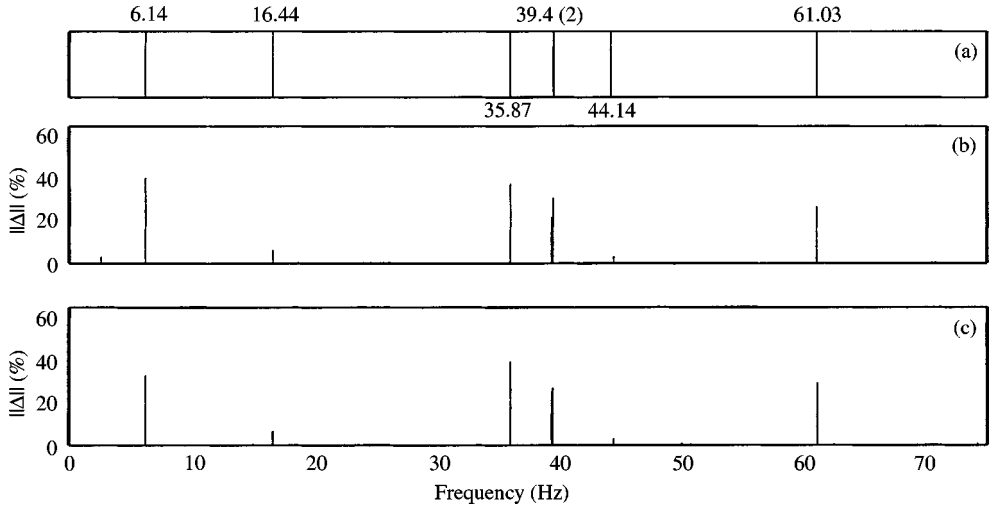

Figure 18. (a) Force appropriation-based frequencies; (b) ARX(20, 20)-based frequencies and dispersion norms; (c) ARMAX(16, 16, 1)-based frequencies and dispersion norms (10% added colour noise).

The ARMAX(16, 16, 1)-based frequency response magnitude curves are in close agreement with those obtained in the previous test cases, and the model-based simulations remain in agreement with the actual (measured) structural vibrations.

3.3.2. ARX identification

The estimation of ARX(k, k) models with $k = 5, 6, 7, \ldots$ reveals 'slow' convergence toward frequency 'stabilisation'. For the additional, approximate 'stabilisation' of modal dispersions, combined with accurate estimation of modal damping, $k \geqslant 20$ is required. The problems with 'extraneous' frequencies tending to stabilise are, like in the ARMAX case, more pronounced, especially for the two noise frequencies. Model adequacy (based upon the BIC) is achieved for the ARX(16, 16) model; yet the ARX(20, 20) is selected as somewhat more accurate. The degree of overdetermination in this case is 329%, and the number of data samples per estimated model parameter (SPP) is 33.5.

The ARX(20, 20)-based modal parameters are, for the considered frequency range, presented in Table 5, along with their corresponding dispersion matrix norms. Once again, the results clearly indicate the presence of seven significant ($\|\Delta\| > 3\%$) modes, which are in close agreement with those identified in the previous test cases and also obtained through force appropriation (also see Fig. 18). The estimated damping ratios are all in good agreement with those provided by force appropriation. All 'extraneous' modes, including the two noise modes at 30 and 50 Hz, are clearly identified as such by the digital dispersion analysis (DA).

The ARX(20, 20)-based frequency response magnitude curves are in close agreement with those obtained in the previous test cases, and the model-based simulations remain in agreement with the actual (measured) structural vibrations. In comparing the ARX and ARMAX model performance in this case, it is worth observing that the ARMAX models achieve much better fits than their ARX counterparts; a fact also reflected in their corresponding BIC values which are, despite their increased parametrisation, lower. It should be, within this context, especially noted that the ARMAX(16, 16, 1) model achieves a BIC value that is better than those of all considered ARX models.

3.3.3. ERA identification

'Lower' order models prove inadequate in this case as well, in particular in identifying both of the structure's closely spaced modes (modes 4 and 5). Frequency stabilisation is, on the other hand, achieved for model orders of 44 or higher. Yet, it is once again problematic, as several 'extraneous' (including the noise) modes 'stabilise' as well. In any case, frequency stabilisation, combined with singular value information, leads to a selected state-space model of order $n = 44$. This is characterised by degree of overdetermination equal to 214%. The number of data samples per estimated model parameter (SPP) is very low, at 4.8.

The ERA-based modal parameters are, for the considered frequency range, presented in Table 5, along with the corresponding modal amplitude coherence (MAC) values. The first six structural modes are estimated, although the distance between modes 4 and 5 is increased and the damping of modes 1 and 4 is overestimated (at 3.71 and 2.22%, respectively). The seventh mode is, once again not properly estimated, although some 'neighbouring' frequencies are obtained. Like in the previous test cases, however, the most significant problem is the distinction of the structural from 'extraneous' modes in view of the fact that the latter appear characterised by high MAC values as well (Table 5). This is so for the two noise modes too, which are thus impossible to detect as such.

4. DISCUSSION

Some general comments that may be made regarding each one of the methods follow.

4.1. THE MIMO LMS-ARMAX METHOD

The LMS-ARMAX method was shown to be effective in accurately identifying the dynamics of the structure under study based upon the 2-input 3-output measurements. The MIMO ARMAX representation was shown to be both 'economical' and appropriate for structural identification, and the method had no difficulty with either the dimensionality of the problem or the high model orders used. The guaranteed stability version proved both necessary and effective, statistical order selection criteria (such as the BIC) useful and the digital dispersion analysis (DA) valuable in distinguishing structural from 'extraneous' (including noise) modes.

4.2. THE MIMO ARX METHOD

The ARX version was shown to be effective as well, although (due to the nature of the ARX representation) it generally had to resort to higher-order models and a consequently increased number of 'extraneous' modes. 'Stabilisation' may be slower in this case, and the problem of 'extraneous' mode 'stabilisation' more pronounced.

4.3. THE ERA

The ERA was shown to be somewhat less accurate than the previous methods, in particular in identifying the structure's closely spaced and the highest frequency modes. Furthermore, the estimated models were occasionally found to be unstable. Frequency 'stabilisation' may be somewhat slow in this case as well, and the problem of 'extraneous' mode 'stabilisation' and modal 'splitting' pronounced. Model order determination was shown to be hard to accomplish via singular value diagrams, while the MAC was not effective in distinguishing structural from 'extraneous' modes. Finally, the use of high-order models was found to be potentially problematic because of the large number of state-space parameters necessary and the resulting low number of data samples per estimated parameter (SPP).

Specific remarks on the important issues set forth in the Introduction of this part of the paper follow.

(i) *Higher-dimensional problems.* Neither the dimensionality of the problem nor the high-order models used caused particular difficulties. Exceptions to this were observed with the ERA which occasionally provided unstable models and also led to low numbers of samples per parameter (SPP) when attempting to fit higher-order models.

(ii) *Estimation of closely spaced modes.* With appropriate overdetermination, all modes, including the two closely spaced ones, were accurately identified. The ERA achieved somewhat reduced accuracy, especially with regard to one of the closely spaced modes, and exhibited difficulty in obtaining the seventh mode.

(iii) *Estimation of 'local' modes.* No difficulty was encountered with the accurate estimation of the 'local' tail mode from 'remote' measurements.

(iv) *Estimation of light modal damping.* No difficulty was encountered.

(v) *Model overdetermination.* Significant model overdetermination was found to be necessary for accurate identification; this was particularly true with the ARX method. Overdetermination may be nevertheless bound by the need to maintain the SPP above a certain limit; this was particularly evident with the ERA which was forced to low SPP values. Overdetermination was unambiguously dictated by statistical criteria such as the BIC (LMS-ARMAX and ARX methods), which led to the neighbourhood of the selected model and was found to be useful for model order selection. Singular-value diagrams (ERA) were found to be less effective. 'Stabilisation' diagrams proved useful, but 'stabilisation' may be slow and phenomena such as the 'stabilisation' of 'extraneous' modes and modal 'splitting' may pose difficulties.

(vi) *Distinction of structural from 'extraneous' modes.* Given the need for significant overdetermination, the ability to distinguish structural from 'extraneous' modes is of paramount importance. 'Stabilisation' diagrams and the MAC were found to be of limited use in this context. The dispersion analysis (DA) methodology proved to be useful, and was also effective in distinguishing the noise frequencies.

(vii) *Estimation under various noise environments.* Increases in the level of noise were shown to lead to increases in the required level of model overdetermination. The most serious difficulty then is the distinction of structural from 'extraneous' modes (see previous remark). It was indicated that the level of difficulty may increase further when dealing with colour noise.

(viii) *Suitability of discrete-time representations.* ARMAX representations, which account for the presence of noise through their MA part, were found to be more appropriate and parsimonious than their pure ARX counterparts. This was reflected in their resulting lower degrees of overdetermination and also in their better achievable fits: the latter were often translated into lower BIC values as well, despite the ARMAX representations' higher parametrisation complexity. The state-space representations employed did not (explicitly) account for the presence of noise, while their overdetermination quickly led to low SPP values.

5. CONCLUDING REMARKS

(1) A comprehensive MIMO LMS-ARMAX method was introduced. This method features the following.

- Vector ARMAX representations that explicitly account for noise effects and lead to lower overdetermination and effective identification.

- LMS parameter estimation featuring modest computational complexity, high accuracy, and a mathematically guaranteed algorithmic and model stability version, and thus the capability to handle higher-dimensional problems and lightly damped structures.
- Model order selection via statistical (such as the BIC) criteria.
- Accurate modal parameter extraction and effective distinction of structural from 'extraneous' modes via a digital dispersion analysis (DA) methodology.

(2) The LMS-ARMAX method's effectiveness was verified via its application to the modal identification of a scale aircraft skeleton structure characterised by a pair of closely spaced modes as well as a 'local' mode. The method provided stable models and high-quality modal estimates in the cases of added white and colour noise. A number of observations on determining the necessary model overdetermination and the distinction of structural modes were made.

(3) Critical comparisons of the LMS-ARMAX method with a pure ARX version and the Eigensystem Realisation Algorithm (ERA) were also made. The ARMAX/ARX methods were shown to achieve superior accuracy in all considered cases, with the LMS-ARMAX method leading to more parsimonious representations (somewhat lower overdetermination) and overall better model fits. This was frequently reflected in lower BIC values, despite the ARMAX representation's higher parametrisation. The ERA lagged behind in terms of achievable accuracy and the distinction of structural modes via the MAC.

ACKNOWLEDGEMENTS

The authors are grateful to Maurice Goursat of INRIA (Rocquencourt, France) and Thierry Biolchini of SOPEMEA (Velizy, France) for providing the experimental data. This part of the study was partially supported by the Plato French–Greek Research and Technology Collaboration Program (Project #96046).

REFERENCES

1. S. D. Fassois 2000 *Mechanical Systems and Signal Processing* **15**, 723–735. MIMO LMS-ARMAX identification of vibrating structures—Part I: the method.
2. J.-N. Juang and R. S. Pappa 1985 *Journal of Guidance, Control and Dynamics* **8**, 620–627. An eigensystem realization algorithm (ERA) for modal parameter identification and model reduction.
3. J.-N. Juang 1994 *Applied System Identification*. Englewood Cliffs, NJ: Prentice-Hall PTR.
4. A. Florakis, S. D. Fassois and F. M. Hemez 1998 *Proceedings of the International Modal Analysis Conference*, 137–143. Critical assessment of MIMO structural identification methods: ARX and ARMAX schemes.
5. R. S. Pappa 1990 *Sound and Vibration*, 16–21. Identification challenges in large space structures.
6. E. Balmes and J. R. Wright 1997 *Proceedings of DETC'97, ASME Design Engineering Technical Conferences*, Sacramento, CA, Paper DETC97/VIB-4255. GARTEUR Group on ground vibration testing—results from the test of a single structure by 12 laboratories in Europe.
7. S. D. Fassois, K. F. Eman and S. M. Wu 1990 *Journal of Dynamic Systems, Measurement, and Control* **112**, 1–9. Sensitivity analysis of the discrete-to-continuous dynamic system transformation.
8. S. M. Kay 1988 *Modern Spectral Estimation: Theory and Application*. Englewood Cliffs, NJ: Prentice-Hall.

APPENDIX A: THE EIGENSYSTEM REALISATION ALGORITHM (ERA)

The Eigensystem Realisation Algorithm (ERA) utilises impulse vibration response data to identify a state-space model of the form

$$\begin{aligned} \mathbf{z}[t+1] &= \mathbf{A}\cdot\mathbf{z}[t] + \mathbf{B}\cdot\mathbf{x}[t] \\ \mathbf{y}[t] &= \mathbf{C}\cdot\mathbf{z}[t] + \mathbf{D}\cdot\mathbf{x}[t] \end{aligned} \tag{A1}$$

in which $\mathbf{x}[t]$ $(r\times 1)$, $\mathbf{y}[t]$ $(p\times 1)$ and $\mathbf{z}[t]$ $(n\times 1)$ are the input, output and state vectors, respectively, and $\mathbf{A}$, $\mathbf{B}$, $\mathbf{C}$, $\mathbf{D}$, the state, input, output and direct transmission matrices, respectively.

A brief outline of the method follows (see reference [3] for details). Let $\{\mathbf{Y}_0, \mathbf{Y}_1, \ldots, \mathbf{Y}_{N-1}\}$ designate the system's observed Markov parameters, with each $\mathbf{Y}_t(p\times r)$ (r, p, n indicating the dimensionality of the input, output and state vectors, respectively) being of the form

$$\mathbf{Y}_t \triangleq [\mathbf{y}^1[t]\ \mathbf{y}^2[t]\ \cdots\ \mathbf{y}^r[t]] \tag{A2}$$

with $\mathbf{y}^i[t]$ $(p\times 1)$ indicating the response vector due to an impulse excitation at the ith input. Next form the generalised $\alpha\cdot p\times\beta\cdot r$ Hankel matrix as

$$\mathbf{H}[k-1] = \begin{bmatrix} \mathbf{Y}_k & \mathbf{Y}_{k+1} & \cdots & \mathbf{Y}_{k+\beta-1} \\ \mathbf{Y}_{k+1} & \mathbf{Y}_{k+2} & \cdots & \mathbf{Y}_{k+\beta} \\ \vdots & \vdots & & \vdots \\ \mathbf{Y}_{k+\alpha-1} & \mathbf{Y}_{k+\alpha} & \cdots & \mathbf{Y}_{k+\alpha+\beta-2} \end{bmatrix} \tag{A3}$$

which is of rank n, provided that $\alpha \geqslant n$, $\beta \geqslant n$ (α, β constitute the method's 'design parameters'; their proper selection may require a number of trials).

The singular value decomposition of $\mathbf{H}[0]$ gives ($\alpha p \geqslant \beta r$),

$$\mathbf{H}[0] = \mathbf{R}\cdot\mathbf{\Sigma}\cdot\mathbf{S}^T \tag{A4}$$

where $\mathbf{R}$ $(\alpha\cdot p\times\alpha\cdot p)$, $\mathbf{S}$ $(\beta\cdot r\times\beta\cdot r)$ are orthonormal matrices ($\mathbf{R}^T\mathbf{R} = \mathbf{I}_{\alpha p}$, $\mathbf{S}^T\mathbf{S} = \mathbf{I}_{\beta r}$, with $\mathbf{I}$ representing identity matrix of the indicated dimension). The columns of $\mathbf{R}$ and $\mathbf{S}$ are the left and right singular vectors, respectively. The matrix $\mathbf{\Sigma}$ $(\alpha\cdot p\times\beta\cdot r)$ contains the system's singular values σ_i. Theoretically, the nth order system has exactly n non-zero singular values, say $\sigma_1 \geqslant \sigma_2 \geqslant \cdots \geqslant \sigma_n > 0$. Thus, the $\mathbf{\Sigma}$, $\mathbf{R}$, $\mathbf{S}$ matrices may be partitioned as

$$\mathbf{\Sigma} = \begin{bmatrix} \mathbf{\Sigma}_n & \mathbf{0} \\ \mathbf{0} & \mathbf{0} \end{bmatrix}, \quad \mathbf{R} = [\mathbf{R}_n\ \bar{\mathbf{R}}], \quad \mathbf{S} = [\mathbf{S}_n\ \bar{\mathbf{S}}] \tag{A5}$$

with $\mathbf{\Sigma}_n \triangleq \mathrm{diag}(\sigma_1, \sigma_2, \ldots, \sigma_n)$ (diag representing diagonal matrix with the indicated elements), and $\mathbf{R}_n$, $\mathbf{S}_n$ being composed of the corresponding n columns of $\mathbf{R}$, $\mathbf{S}$, respectively.

The state-space matrices may then be estimated as

$$\hat{\mathbf{A}} = \mathbf{\Sigma}_n^{-1/2}\cdot\mathbf{R}_n^T\cdot\mathbf{H}[1]\cdot\mathbf{S}_n\cdot\mathbf{\Sigma}_n^{-1/2} \tag{A6}$$

$$\hat{\mathbf{B}} = \mathbf{\Sigma}_n^{1/2}\cdot\mathbf{S}_n^T\cdot\mathbf{E}_r \tag{A7}$$

$$\hat{\mathbf{C}} = \mathbf{E}_p^T\cdot\mathbf{R}_n\cdot\mathbf{\Sigma}_n^{1/2} \tag{A8}$$

while $\hat{\mathbf{D}} = \mathbf{Y}_0$. In the above $\mathbf{E}_p^T \triangleq [\mathbf{I}_p\,\mathbf{0}_p\cdots\mathbf{0}_p]$, $\mathbf{E}_r^T \triangleq [\mathbf{I}_r\,\mathbf{0}_r\cdots\mathbf{0}_r]$ with $\mathbf{0}_i$ representing a null $i\times i$ matrix.

The discrete-time eigenvalues (system poles) are estimated from the characteristic equation,

$$\det[\lambda\mathbf{I}_n - \mathbf{A}] = 0 \tag{A9}$$

following which the (**A**, **B**, **C**) matrices may be transformed into modal coordinates as ($\mathbf{\Lambda}$, $\mathbf{\Psi}^{-1}\mathbf{B}$, $\mathbf{C\Psi}$), with $\mathbf{\Lambda} \triangleq \text{diag}(\lambda_1, \ldots, \lambda_n)$ and $\mathbf{\Psi} \triangleq [\boldsymbol{\psi}_1 \boldsymbol{\psi}_2 \cdots \boldsymbol{\psi}_n]$ being the corresponding eigenvector matrix. The matrix $\mathbf{\Psi}^{-1}\mathbf{B}$ provides the initial modal amplitudes (modal participation factors) and the matrix $\mathbf{C\Psi}$ the mode shapes at the sensor points.

The determination of the true structural modes (among a higher number of modes generally identified) is based upon the modal amplitude coherence (MAC). The value of the MAC for the *i*th eigenvalue is defined as the normalised dot product between the vectors $\bar{\mathbf{q}}_i$ and $\hat{\mathbf{q}}_i$,

$$MAC_i = \frac{|\bar{\mathbf{q}}_i^* \cdot \hat{\mathbf{q}}_i|}{|\bar{\mathbf{q}}_i^* \cdot \bar{\mathbf{q}}_i|^{1/2} |\hat{\mathbf{q}}_i^* \cdot \hat{\mathbf{q}}_i|^{1/2}} \tag{A10}$$

with '$*$' indicating complex conjugate transposition $\bar{\mathbf{q}}_i$ ($\beta \cdot r \times 1$) is obtained by transposing the *i*th row of the controllability matrix

$$\bar{\mathbf{Q}}_{ctr} = \mathbf{\Psi}^{-1} \cdot \mathbf{\Sigma}_n^{1/2} \cdot \mathbf{S}_n^T \tag{A11}$$

whereas $\hat{\mathbf{q}}_i$ ($\beta \cdot r \times 1$) is obtained as

$$\hat{\mathbf{q}}_i = [\mathbf{b}_i^T \quad \lambda_i \cdot \mathbf{b}_i^T \; \lambda_i^2 \cdot \mathbf{b}_i^T \; \ldots \; \lambda_i^{\beta-1} \cdot \mathbf{b}_i^T]^T \tag{A12}$$

with $\mathbf{b}_i$ ($r \times 1$) being the transposed *i*th row of the matrix $\mathbf{\Psi}^{-1}\mathbf{B}$. MAC values are obviously confined in the interval [0, 1]. Eigenvalues (and thus corresponding modes) with MAC values close to unity are classified as structural; otherwise, as 'extraneous' (false).